LETTERS

The effect of water on the electrical conductivity of olivine

Duojun Wang[1,2,3], Mainak Mookherjee[3], Yousheng Xu[3,4] & Shun-ichiro Karato[3]

It is well known that water (as a source of hydrogen) affects the physical and chemical properties of minerals—for example, plastic deformation[1–3] and melting temperature[4]—and accordingly plays an important role in the dynamics and geochemical evolution of the Earth. Estimating the water content of the Earth's mantle by direct sampling provides only a limited data set from shallow regions (<200 km depth)[5]. Geophysical observations such as electrical conductivity are considered to be sensitive to water content[6], but there has been no experimental study to determine the effect of water on the electrical conductivity of olivine, the most abundant mineral in the Earth's mantle. Here we report a laboratory study of the dependence of the electrical conductivity of olivine aggregates on water content at high temperature and pressure. The electrical conductivity of synthetic polycrystalline olivine was determined from a.c. impedance measurements at a pressure of 4 GPa for a temperature range of 873–1,273 K for water contents of 0.01–0.08 wt%. The results show that the electrical conductivity is strongly dependent on water content but depends only modestly on temperature. The water content dependence of conductivity is best explained by a model in which electrical conduction is due to the motion of free protons. A comparison of the laboratory data with geophysical observations[7–10] suggests that the typical oceanic asthenosphere contains ~10^{-2} wt% water, whereas the water content in the continental upper mantle is less than ~10^{-3} wt%.

Karato[6] proposed that hydrogen enhances electrical conductivity in olivine either directly through charge transport by protons or indirectly through enhancement of ionic conductivity by Mg-Fe diffusion. Although this hypothesis has been used to interpret results of geophysical measurements of electrical conductivity[10–13], there has been no experimental data to test this hypothesis. In fact, the recent study of wadsleyite and ringwoodite[14] does not entirely support Karato's hypothesis: electrical conduction in these minerals (with hydrogen) occurs through the motion of free protons—but not of all protons as Karato[6] assumed (protons bound in the M-sites do not contribute to conductivity directly). If this is the case for olivine, then the results of these previous studies will be invalidated, and the issue of estimating water content from electrical conductivity would have to be revisited. Consequently, we have conducted an experimental study of the influence of hydrogen on electrical conductivity in olivine, and applied the results to infer the water (hydrogen) content of the upper mantle. In this Letter we report the first results and present discussions of their implications.

The starting material was San Carlos olivine. Inclusion-free, clear crystals were selected, and crushed into fine grains. Grains with different sizes were sorted by the sedimentation method. We added ~2% orthopyroxene to control the silica activity. A powder sample is packed in a nickel capsule and hot-pressed at ~4 GPa, 1,373–1,473 K for ~1–3 h using a Kawai-type multianvil press (the presence of NiO was confirmed after the synthesis). A small amount of water was added by the decomposition of a talc+brucite mixture. Water contents of samples were measured both before and after each measurement of electrical conductivity by Fourier-transform infrared (FT-IR) spectroscopy. The calibration given in ref. 15 was used to calculate the water content of olivine grains from infrared absorption; corrections were made for the contribution of 'grain-boundary' water (see Methods). Grain sizes of hot-pressed samples are ~10–30 μm. The distribution of crystallographic orientations is nearly random, as determined by electron backscatter diffraction measurements.

Figure 1 shows the sample assembly for electrical conductivity measurements. A disk-shaped sample (~1.6 mm diameter, ~0.4 mm thickness) is placed between two Ni electrodes that are surrounded by alumina rings. All metallic components in the sample assembly are made of Ni to make sure that the oxygen fugacity during the measurements is close to that of the Ni–NiO buffer at which

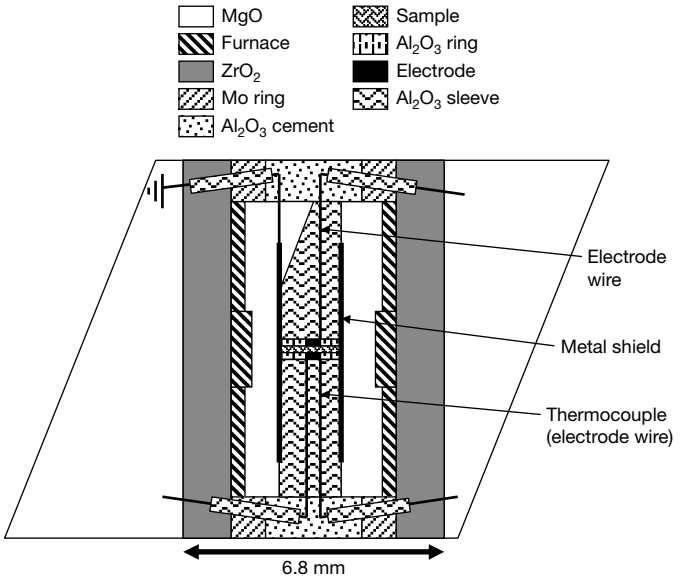

Figure 1 | The sample assembly for electrical conductivity measurements at high pressure. A polycrystalline disk-shaped sample (diameter 1.6 mm, thickness 0.4 mm) is inserted between two alumina rods that contain Ni electrodes. Note that a thermocouple is in contact with the sample so that the temperature at which conductivity is measured can be determined with a small uncertainty. The response of the sample to an a.c. voltage is recorded as a function of frequency to obtain the complex impedance. The resistance is calculated from the complex impedance. The sample space is separated from the furnace by a thin cylinder of Ni that acts as a shield to minimize the noise and the leak current.

[1]Institute of Geochemistry, Chinese Academy of Sciences, Guiyang 550002, China. [2]Institute of Geology, China Earthquake Administration, Beijing 100029, China. [3]Department of Geology and Geophysics, Yale University, New Haven, Connecticut 06520, USA. [4]Department of Mathematics, University of Connecticut, Storr, Connecticut 06269, USA.

hot-pressed specimens were equilibrated. A cylindrical Ni foil is placed between the sample and the furnace to minimize the leakage currents (for details, see ref. 16). The temperature was measured by a W5%Re-W26%Re thermocouple that is placed next to the sample and is also used as one of the electrodes. The temperature reading is stable better than ~10 K during one measurement. The complex impedances of samples were determined by a Solartron 1260 impedance/gain phase analyser at 4 GPa and 873–1,273 K within the frequency range 10^3–10^6 Hz with a voltage of 0.1 V. The choice of relatively low voltage and a high frequency range was made to minimize the hydrogen loss during an experiment. All the data shown here are from measurements in which water loss (calculated from water content before and after the experiment) is less than ~20%. A complete list of the results is provided in a Table in Supplementary Information 1. The conductivity values were calculated from the complex impedance of samples. The results are shown in Fig. 2. The error in the conductivity measurement is largely due to the resistance fit and are ±5%, the errors in temperature measurements are ±10 K or better, and the major errors are those for water content and are ±20% (see Methods).

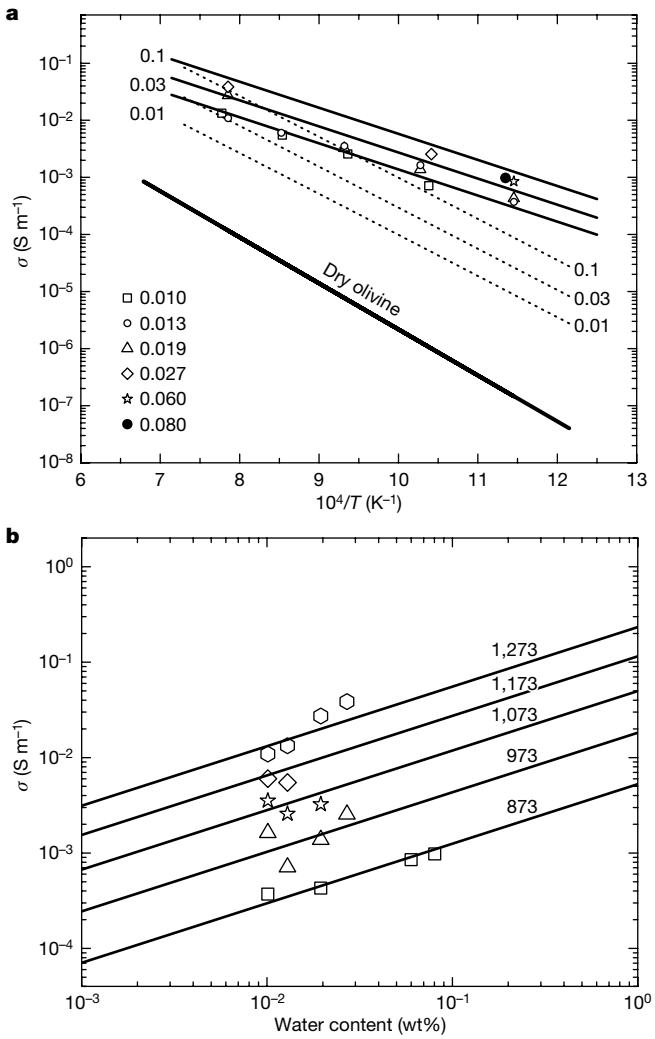

Figure 2 | Electrical conductivity versus inverse temperature and water content. **a**, A plot of electrical conductivity (σ) versus inverse temperature. The numbers next to each line indicate the water content (in wt%). Solid lines with numbers are the results of multilinear regression from all the data. Each symbol represents the data corresponding to a given water content (in wt%). The broken lines show the conductivity values calculated from water diffusion coefficients determined by Kohlstedt and Mackwell[22] using the model by Karato[6], and the conductivity for 'dry' olivine[20]. Both the magnitude and the slope from the present study are different from those of 'dry' olivine and the trend calculated using the Karato model, indicating that the charge carrier corresponding to the present study is different from those in the previous studies (neutral hydrogen-defect at M-sites for the Karato model, Fe^{3+} for 'dry' olivine). **b**, A plot of electrical conductivity versus water content. The fit of the data to a model equation yields $r = 0.62 \pm 0.15$. The numbers along each line represent the temperature in K. A relatively large error for r is due to the fact that only a narrow range of water content can be explored for olivine due to the relatively small hydrogen solubility, and to a large error in the estimate of water content from FT-IR (see Methods). Each symbol corresponds to the data for a given temperature (in K).

Electrical conductivities of a mineral containing both hydrogen and iron can be written as:

$$\sigma = \sigma_{Fe} + \sigma_H \quad (1)$$

where σ_{Fe} is the electrical conductivity due to ferric iron, and σ_H is the electrical conductivity due to hydrogen. σ_H may be written as:

$$\sigma_H = AC_w^r \exp\left(-\frac{H^*}{RT}\right) \quad (2)$$

where we used a relation that the electrical conductivity is proportional to the concentration of charged species and their mobility (Nernst–Einstein relation), and the concentration of charged species is proportional to C_w^r, where C_w is the water content, A and r are constants, H^* is the activation enthalpy, R is the gas constant and T is temperature. The results are summarized in Table 1 together with the results for 'dry' olivine. The errors in estimated parameters are for one standard deviation, and errors in temperature, conductivity and water content measurements are included in the error estimate of these parameters. The range of grain sizes is too narrow to constrain any grain-size sensitivity, but a comparison of the present results with the results on a coarse-grained dunite[17] (~1 mm grain size) suggests that the grain-size effect, if any, is small.

For hydrogen-free ('dry') olivine, electrical conductivity (σ_{dry}) is due mainly to the migration of electron holes that are created by ferric iron and $\sigma_{dry} \approx \sigma_{Fe}$ (refs 18, 19; note, however, that σ_{Fe} is in general dependent on hydrogen (water) content and $\sigma_{dry} = \lim_{C_w \to 0} \sigma_{Fe}$). The values of electrical conductivity in our hydrogen-bearing olivine are significantly higher than those of hydrogen-free ('dry') olivine[20] (Fig. 2a). Also, the activation enthalpy for 'dry' olivine (~154 kJ mol^{-1}) is much higher than that of 'wet' olivine (~87 ± 5 kJ mol^{-1}), and there are very small pressure effects on electrical conductivity[21]. Therefore, the conduction mechanism is different between 'wet' and 'dry' samples. For dry olivine samples, the conduction mechanism is considered to be the migration of electron holes[18,19]. However, for 'wet' olivine samples, it should be due to a different charged species, hydrogen: $\sigma_{wet} \approx \sigma_H$.

Let us examine how hydrogen enhances electrical conductivity. Karato[6] assumed that the electrical conductivity in olivine containing hydrogen is dominated by the diffusion of hydrogen, and used the experimental data on hydrogen diffusion and solubility to calculate the electrical conductivity. The data that Karato[6] used were chemical diffusion of hydrogen, but a later analysis by Kohlstedt and Mackwell[22] showed that the data on chemical diffusion roughly correspond to self diffusion of protons (corrected by a factor of 2). Consequently, we use the data by Kohlstedt and Mackwell[22] and

Table 1 | Parameter values for electrical conductivity of olivine

Olivine conditions	$\log_{10}[A$ (S m^{-1})]	r	H^* (kJ mol^{-1})
Wet	3.0 ± 0.4	0.62 ± 0.15	87 ± 5
Dry	2.4	0	154

The relation $\sigma = AC_w^r \exp(-H^*/RT)$ is used. Errors are for one standard deviation, and include the contribution of errors in individual measurements (error in temperature, water content and conductivity). The data for 'dry' conditions are from ref. 20. The electrical conductivity under 'dry' conditions corresponds to conductivity due to ferric iron at zero hydrogen content ($\sigma_{dry} = \lim_{C_w \to 0} \sigma_{Fe}$).

the Nernst–Einstein equation to calculate electrical conductivity in olivine. The conductivity of an aggregate is calculated from the single crystal diffusion data by taking a Hashin–Shtrikman average[23]. The results are compared with our experimental data. We note that the absolute values of electrical conductivity calculated from the Karato[6] model are significantly lower than the actually measured values at low temperatures, whereas the measured values are in good agreement with the Karato model at high temperatures. Also, the activation enthalpy of electrical conductivity ($87 \pm 5\,\mathrm{kJ\,mol^{-1}}$) is significantly smaller than that of diffusion of hydrogen ($150 \pm 30\,\mathrm{kJ\,mol^{-1}}$)[22] (Methods). Therefore we conclude that the mechanism of electrical conductivity in olivine is different from Karato's model[6].

Huang *et al.*[14] reached a similar conclusion, and suggested electrical conduction by free protons produced by an ionization reaction:

$$(2\mathrm{H})_{\mathrm{M}}^{\times} \Leftrightarrow \mathrm{H}'_{\mathrm{M}} + \mathrm{H}^{\bullet} \quad (3)$$

where H'_{M} is a proton trapped at an M-site vacancy and $\mathrm{H}^{\bullet}$ is a free proton. This mechanism predicts $r = 0.75$ (for the charge neutrality condition of $[\mathrm{H}'_{\mathrm{M}}] = [\mathrm{Fe}^{\bullet}_{\mathrm{M}}]$) or 0.50 (for $2[\mathrm{V}''_{\mathrm{M}}] = [\mathrm{Fe}^{\bullet}_{\mathrm{M}}]$ where $\mathrm{V}''_{\mathrm{M}}$ is a vacancy at an M-site) as opposed to $r = 1$ for the Karato model[6]. The value of r in our study is 0.62 ± 0.15 (Fig. 2b), which is significantly lower than the Karato model[6], and is consistent with the free proton model, although the errors in r are admittedly large (due mainly to the large errors in water content measurements).

An alternative mechanism by which hydrogen may enhance electrical conductivity is through the enhancement of diffusion of Mg (Fe). However, a recent experimental study[24] indicates that the influence of conduction by diffusion of Mg (Fe) is small.

The chemical conditions of our experiments (that is, oxygen fugacity and oxide activity) are nearly identical to those in the Earth's upper mantle. The pressure (4 GPa) at which electrical conductivity was measured corresponds to the typical upper asthenosphere (~120 km depth). However, the temperature range used in our experiments (873–1,273 K) is lower than a typical temperature of the asthenosphere (~1,600–1,700 K). Therefore we extrapolate our results in terms of temperature and compare the results with some of the geophysical observations of electrical conductivity in the upper mantle (~100–200 km) (Fig. 3). This extrapolation causes only small uncertainties because the activation enthalpy is well constrained by the present study (see Table 1 and Methods) and the extrapolation in $1/T$ space is not large compared to the range of $1/T$ space in which the measurements were made. The electrical conductivity of the oceanic asthenosphere is typically $\sim 10^{-1}\,\mathrm{S\,m^{-1}}$ (refs 9–11), which corresponds to a water content of $\sim 0.8 \times 10^{-2}$ wt% (~1,500 p.p.m. H/Si) (error is ~±50%). This value agrees well with the estimated water content from the composition of mid-ocean ridge basalt (see ref. 25 for a review). However, geophysical observations[7–11] also show that electrical conductivity has a large regional variation. The electrical conductivity in the continental upper mantle is typically lower, on the order of $\sim 10^{-2}\,\mathrm{S\,m^{-1}}$ (refs 7, 8). These values correspond to a significantly lower water content, on the order of $\sim 10^{-3}$ wt% or lower.

We also note that if hydrogen is indeed responsible for electrical conductivity in hydrogen-rich olivine, and if electrical conduction occurs mostly through grains, then one would expect anisotropy in electrical conductivity if olivine assumes strong lattice-preferred orientation. Some geophysical observations suggest anisotropy in electrical conductivity in the upper mantle[26,27], but a quantitative assessment of anisotropy in electrical conductivity will require an experimental study on strongly textured olivine aggregates.

We conclude that our experimental study has established a solid foundation for the use of geophysically inferred electrical conductivity to infer water content (and temperature) in the upper mantle of the Earth. Using observations of geomagnetic field from networks including ocean-bottom electro-magnetometers, high-resolution electrical conductivity profiles in three dimensions are becoming available. A combination of these results with laboratory studies will provide important data to constrain the distribution of hydrogen in the upper mantle of the Earth, which will provide a clue to the evolution of this region of our planet.

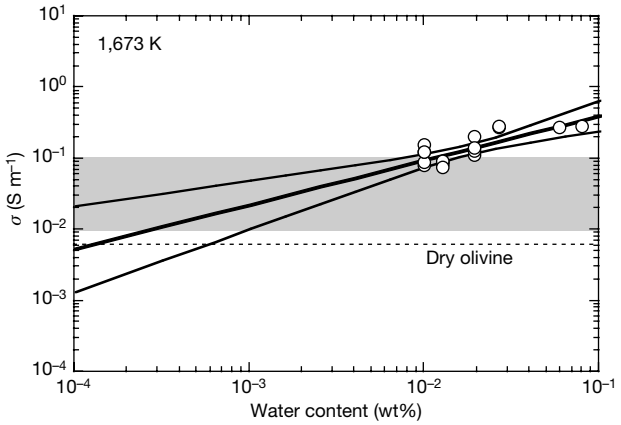

Figure 3 | Comparison of the conductivity of hydrogen-bearing olivine with geophysically inferred electrical conductivity for the asthenosphere. Symbols show the calculated conductivity at $T = 1{,}673$ K from our results. The thick line indicates a best-fit line for the data, and the two thinner curves show the error envelope corresponding to one standard deviation. The electrical conductivity of the oceanic asthenosphere is typically $\sim 10^{-1}\,\mathrm{S\,m^{-1}}$ (refs 10, 11, 30), whereas that in the continental deep upper mantle (in the same depth range) is $\sim 10^{-2}\,\mathrm{S\,m^{-1}}$ (refs 7, 8). Shown also (horizontal broken line) is the electrical conductivity of hydrogen-free olivine. The thick horizontal grey bar indicates a range of typical values of electrical conductivity of the upper mantle (~100–200 km). We conclude that for the oceanic asthenosphere, the water content is estimated to be $\sim 0.8 \times 10^{-2}$ wt% (~1,500 p.p.m. H/Si), which is in excellent agreement with geochemical inference[25]. In contrast, the water content in the continental upper mantle is significantly lower, and the conductivity values there are consistent with those of 'dry' olivine.

METHODS

Determination of water content. The water (hydrogen) content of samples was measured on polycrystalline samples using FT-IR absorption spectroscopy. An IR absorption by a polycrystalline sample is caused by OH-related species in grains as well as these species on grain boundaries. Our IR absorption spectra contain both a broad peak centred at ~3,400 $\mathrm{cm^{-1}}$ and sharp peaks at ~3,500–3,600 $\mathrm{cm^{-1}}$. Previous results suggest that a broad peak observed in polycrystalline samples is due to water on grain boundaries[3] or to quenched melt[28]. Consequently, we subtracted a broad peak at ~3,400 $\mathrm{cm^{-1}}$ from the original spectrum to estimate the water content in the grains in each sample (see Supplementary Information 2). The water content in the grains in a polycrystalline sample estimated in this way agrees reasonably well with the solubility of water reported in ref. 29 (with an error of ±20%).

Activation enthalpy. The activation enthalpy determined in our experiments includes the temperature dependence of the concentration of defects ($\propto \exp\left(-\frac{H_{\mathrm{f}}^{*}}{RT}\right)$, where H_{f}^{*} is the enthalpy for defect formation) and the temperature dependence of the mobility of defects ($\propto \exp\left(-\frac{H_{\mathrm{m}}^{*}}{RT}\right)$, where H_{m}^{*} is the enthalpy for defect mobility). Therefore the activation enthalpy is $H^{*} = H_{\mathrm{f}}^{*} + H_{\mathrm{m}}^{*}$. In our experiments, the total water content in a sample in a series of experiments at various temperatures is kept nearly constant. However, the fraction of charge carrying species, $H^{\bullet}$, may change with temperature (in other words, H_{f}^{*} in our case corresponds to the enthalpy change associated with the reaction given in equation (3)). Such is probably the case in the Earth's mantle where minerals are under-saturated with water and the system is nearly closed. Consequently, the application of our data on the activation enthalpy to the Earth's interior is probably justified.

Note, however, that the total hydrogen content in diffusion experiments changes with temperature. The difference in the activation enthalpy between diffusion experiments ($150 \pm 30\,\mathrm{kJ\,mol^{-1}}$) and electrical conductivity ($87 \pm 5\,\mathrm{kJ\,mol^{-1}}$) could be due to the temperature dependence of hydrogen solubility, which is proportional to $\exp\left(-\frac{H_{\mathrm{sol}}^{*}}{RT}\right)$ with $H_{\mathrm{sol}}^{*} \approx 50\,\mathrm{kJ\,mol^{-1}}$.

Received 31 March; accepted 11 September 2006.

1. Karato, S. & Jung, H. Effects of pressure on high-temperature dislocation creep in olivine polycrystals. *Phil. Mag. A* **83**, 401–414 (2003).
2. Karato, S., Paterson, M. S. & Fitz Gerald, J. D. Rheology of synthetic olivine aggregates: influence of grain-size and water. *J. Geophys. Res.* **91**, 8151–8176 (1986).
3. Mei, S. & Kohlstedt, D. L. Influence of water on plastic deformation of olivine aggregates, 1. Diffusion creep regime. *J. Geophys. Res.* **105**, 21457–21469 (2000).
4. Kushiro, I., Syono, Y. & Akimoto, S. Melting of a peridotite nodule at high pressures and high water pressures. *J. Geophys. Res.* **73**, 6023–6029 (1968).
5. Bell, D. R. & Rossman, G. R. Water in Earth's mantle: The role of nominally anhydrous minerals. *Science* **255**, 1391–1397 (1992).
6. Karato, S. The role of hydrogen in the electrical conductivity of the upper mantle. *Nature* **347**, 272–273 (1990).
7. Olsen, N. Long-period (30 days - 1 year) electromagnetic sounding and the electrical conductivity of the lower mantle beneath Europe. *Geophys. J. Int.* **138**, 179–187 (1999).
8. Tarits, P., Hautot, S. & Perrier, F. Water in the mantle: Results from electrical conductivity beneath the French Alps. *Geophys. Res. Lett.* **31**, doi:10.1029/2003GL019277 (2004).
9. Evans, R. L. *et al.* Geophysical evidence from the MELT area for compositional control on oceanic plates. *Nature* **437**, 249–252 (2005).
10. Lizarrale, D., Chave, A., Hirth, G. & Schultz, A. Northeastern Pacific mantle conductivity profile from long-period magnetotelluric sounding using Hawaii-to-California cable data. *J. Geophys. Res.* **100**, 17837–17854 (1995).
11. Baba, K., Chave, A. D., Evans, R. L., Hirth, G. & Randall, L. Mantle dynamics beneath the East Pacific Rise at 17°S: Insights from the Mantle Electromagnetic and Tomography (MELT) experiments. *J. Geophys. Res.* **111**, doi:10.1029/2004JB003598 (2006).
12. Simpson, F. & Tommasi, A. Hydrogen diffusivity and electrical anisotropy of a peridotite mantle. *Geophys. J. Int.* **160**, 1092–1102 (2005).
13. Hirth, G., Evans, R. L. & Chave, A. D. Comparison of continental and oceanic mantle electrical conductivity: Is Archean lithosphere dry? *Geochem. Geophys. Geosyst.* **1**, doi:10.1029/2000GC000048 (2000).
14. Huang, X., Xu, Y. & Karato, S. Water content of the mantle transition zone from the electrical conductivity of wadsleyite and ringwoodite. *Nature* **434**, 746–749 (2005).
15. Paterson, M. S. The determination of hydroxyl by infrared absorption in quartz, silicate glass and similar materials. *Bull. Mineral.* **105**, 20–29 (1982).
16. Xu, Y., Poe, B. T., Shankland, T. J. & Rubie, D. C. Electrical conductivity of olivine, wadsleyite, and ringwoodite under upper-mantle conditions. *Science* **280**, 1415–1418 (1998).
17. Wang, D. *Studies on Electrical Properties of Minerals and Rocks Under Defined Thermodynamic Conditions*. Ph.D. thesis, Chinese Acad. Sci. (2004).
18. Karato, S. *Lattice Defects and Transport Properties of Olivine*. M.Sc. thesis, Univ. Tokyo (1974).
19. Schock, R. N., Duba, A. G. & Shankland, T. J. Electrical conduction in olivine. *J. Geophys. Res.* **94**, 5829–5839 (1989).
20. Constable, S., Shankland, T. G. & Duba, A. The electrical conductivity of an isotropic olivine mantle. *J. Geophys. Res.* **97**, 3397–3404 (1992).
21. Xu, Y., Shankland, T. J. & Duba, A. G. Pressure effect on electrical conductivity of mantle olivine. *Phys. Earth Planet. Inter.* **118**, 149–161 (2000).
22. Kohlstedt, D. L. & Mackwell, S. J. Diffusion of hydrogen and intrinsic point defects in olivine. *Z. Phys. Chem.* **207**, 147–162 (1998).
23. Hashin, Z. & Shtrikman, S. A variational approach to the theory of effective magnetic permeability of multiphase materials. *J. Appl. Phys.* **33**, 3125–3131 (1962).
24. Hier-Majumder, S., Anderson, I. M. & Kohlstedt, D. L. Influence of protons on Fe-Mg interdiffusion in olivine. *J. Geophys. Res.* **110**, doi:10.1029/2004JB003292 (2005).
25. Bolfan-Casanova, N. Water in the Earth's mantle. *Mineral. Mag.* **69**, 229–257 (2005).
26. Simpson, F. Intensity and direction of lattice-preferred orientation of olivine: are electrical and seismic anisotropies of the Australian mantle reconcilable? *Earth Planet. Sci. Lett.* **203**, 535–547 (2002).
27. Gatzemeier, A. & Moorkamp, M. 3D modelling of electrical anisotropy from electromagnetic array data: hypothesis testing for different upper mantle conduction mechanisms. *Phys. Earth Planet. Inter.* **149**, 225–242 (2005).
28. Stolper, E. M. Speciation of water in silicate melts. *Geochim. Cosmochim. Acta* **46**, 2609–2620 (1982).
29. Kohlstedt, D. L., Keppler, H. & Rubie, D. C. Solubility of water in the α, β and γ phases of $(Mg,Fe)_2SiO_4$. *Contrib. Mineral. Petrol.* **123**, 345–357 (1996).
30. Ichiki, M. *et al.* Upper mantle conductivity structure of the back-arc region beneath northeastern China. *Geophys. Res. Lett.* **28**, 3773–3776 (2001).

Supplementary Information is linked to the online version of the paper at www.nature.com/nature.

Acknowledgements Z. Jing, Z. Jiang and I. Katayama provided the technical assistance that made this research possible. T. Kawazoe was most helpful with the error estimates. This work was supported by the NSF of China and the NSF of the United States.

Author Contributions S.-i.K. supervised the whole project and completed the paper. The experimental measurements of conductivity and the data analysis were made largely by D.W. and M.M. in collaboration with Y.X.

Author Information Reprints and permissions information is available at www.nature.com/reprints. The authors declare no competing financial interests. Correspondence and requests for materials should be addressed to S.-i.K. (shun-ichiro.karato@yale.edu).